Journal of Alloys and Compounds 509 (2011) 6631–6634

Contents lists available at ScienceDirect

Journal of Alloys and Compounds

journal homepage: www.elsevier.com/locate/jallcom

Analysis of electrical and photoelectrical properties of ZnO/p-InP heterojunction

Yusuf Selim Ocak[a,*], Mustafa Kulakci[b], Rasit Turan[b], Tahsin Kilicoglu[c,d,**], Omer Gullu[d]

[a] Department of Science, Faculty of Education, Dicle University, Diyarbakır, Turkey
[b] Department of Physics, Faculty of Art and Science, METU, Ankara, Turkey
[c] Department of Physics, Faculty of Science, Dicle University, Diyarbakır, Turkey
[d] Department of Physics, Faculty of Art and Science, Batman University, Batman, Turkey

ARTICLE INFO

Article history:
Received 6 December 2010
Received in revised form 17 March 2011
Accepted 18 March 2011
Available online 29 March 2011

Keywords:
Zinc oxide
Indium phosphate
Heterojunction
Solar cell
Sputtering

ABSTRACT

A ZnO/p-InP heterojunction has been fabricated by dc sputtering of ZnO on p-InP. It has been observed that the device has a good rectification. The electrical properties of the device such as ideality factor, barrier height, series resistance have been calculated using its current–voltage (*I*–*V*) measurements between 300 and 380 K with 20 K intervals. The short current density (J_{sc}) and open circuit voltage (V_{oc}) parameters have been determined between 40 and 100 mW/cm^2. The photovoltaic parameters of the device have been also determined under 100 mW/cm^2 and AM1.5 illumination condition.

© 2011 Elsevier B.V. All rights reserved.

1. Introduction

As a direct band gap semiconductor, zinc oxide (ZnO) has band energy of more than 3.3 eV and more than 60 meV of exciton binding energy [1–3]. Transmittance of visible light through the thin ZnO is about 80% [4,5]. ZnO shows better radiation resistance than GaN for possible devices used in space and nuclear applications. Formation of ZnO thin films has been an active field due to its unique semiconductive and piezoelectric dual properties [6]. ZnO films have been prepared by various processes including pulsed laser deposition (PLD) [7], rf and dc magnetron sputtering [8,9], thermal evaporation [10], spray pyrolysis [11,12], sol–gel [13,14], and hydrothermal method [15]. The thin films of ZnO have numerous applications, such as energy efficient windows, solar cells, liquid crystal displays, and other electronic and optoelectronic devices [10,16–18]. For instance, Badran et al. [10] have grown hexagonal-shaped ZnO nanorods on p-silicon substrate via thermal evaporation of metallic zinc powder in the presence of oxygen. They have analyzed the temperature-dependent current–voltage (*I*–*V*) characteristics of p-Si/n-ZnO heterojunction diode.

Because of its 1.35 eV direct band gap, high carrier mobility, high saturation velocity, high absorption coefficient just above the band gap and breakdown voltage [19,20], indium phosphate (InP) is a promising material for high-speed electrical and optoelectronic devices such as photodetectors and solar cells [21,22]. InP solar cells have superior radiation resistance and this has led to considerable work on InP cells for space applications [23]. Many devices based on InP have been produced. For instance, Gullu and Turut [24] have formed quercetin/p-InP organic–inorganic (OI) solar cell via solution-processing method and characterized by current–voltage (*I*–*V*) and capacitance–voltage (*C*–*V*) measurements at room temperature. They also determined the photovoltaic behaviour of the device under 120 l× light intensity.

The main aim of this study is to analyze the electrical and photoelectrical properties of a ZnO/p-InP heterojunction obtained by dc sputtering process. For this aim, we have obtained ZnO/p-InP heterojunction by dc sputtering of ZnO on p-InP wafer. The electrical properties of the device such as ideality factor, barrier height, and series resistance have been determined using *I*–*V* measurements of the diode between 300 and 380 K. The effects of light on electrical properties of the device have been examined under a simulator with 40–100 mW/cm^2 light intensity and 1.5AM global filter. In addition, the photovoltaic properties of the cell have been determined by means of current density–voltage (*J*–*V*) of the cell under 100 mW/cm^2 light intensity.

* Corresponding author at: Department of Science, Faculty of Education, Dicle University, Diyarbakır, Turkey. Tel.: +90 412 248 80 30x8889;
fax: +90 412 248 82 57.
** Corresponding author at: Department of Physics, Faculty of Art and Science, Batman University, Batman, Turkey. Tel.: +90 412 248 85 50; fax: +90 412 248 80 39.
E-mail addresses: yusufselim@gmail.com (Y.S. Ocak), tahsin@dicle.edu.tr, kilicoglutahsin@gmail.com (T. Kilicoglu).

0925-8388/$ – see front matter © 2011 Elsevier B.V. All rights reserved.
doi:10.1016/j.jallcom.2011.03.114

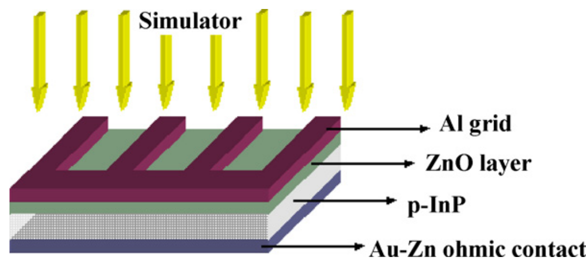

Fig. 1. The illustration of Al/ZnO/p-InP/Zn–Au device under solar simulator.

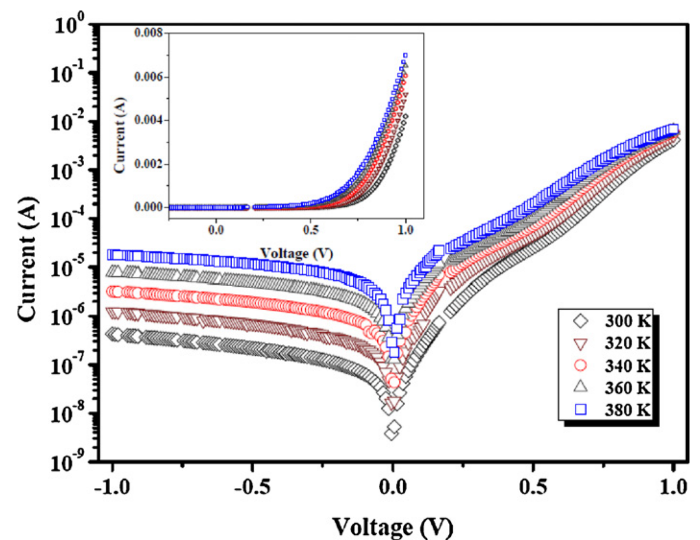

Fig. 2. The experimental dark *I–V* measurements of the Al/ZnO/p-InP heterojunction between 300 and 380 K.

2. Experimental procedures

In this study, the ZnO/p-InP heterojunction was prepared using one side polished (as received from the manufacturer) and Zn doped p-type InP wafer with 3.8×10^{17} cm^{-3} doping density. Firstly, the p-InP wafer was chemically cleaned by 20 s boiling in $3H_2SO_4 + H_2O_2 + H_2O$. The native oxide of the wafer was removed in a HF:H_2O (1:10) solution for 30 s and finally the wafer was rinsed in deionized water and under N_2 atmosphere. The ohmic contact was made by evaporating Au–Zn (90–10%) alloy on the back of the substrate, followed by a temperature treatment at 450 °C for 3 min under N_2 atmosphere. The p-InP/Au–Zn structure was inserted into a vacuum chamber. A ZnO target with a diameter of 2 in. bought from Lesker Company has been used in this study. During the sputtering process, Ar gas was introduced into the chamber and the pressure of the chamber was kept at 5×10^{-3} Torr. The thickness of ZnO thin film was measured as 50 nm using a thickness monitor which was previously calibrated by DEKTAK 6M profilometer for ZnO thin films. The growth rate was about 1 Å/s. After formation of ZnO, Al was thermally evaporated on the structure through a shadow mask which has a grid shape in the vacuum system at 3×10^{-6} Torr as a front contact. The effective area of ZnO/p-InP heterojunction was 0.23 cm^2. The *I–V* measurements of the structure were performed by Keithley 2400 sourcemeter in the range of 300–380 K. A solar simulator with 100 mW/cm^2 illumination and 1.5AM global filter was used for photovoltaic measurements of the device. Fig. 1 presents the illustration of Al/ZnO/p-InP/Zn–Au device under solar simulator.

3. Results and discussion

3.1. Dark current–voltage properties of Al/ZnO/p-InP structure

The experimental dark *I–V* measurements of the Al/ZnO/p-InP heterojunction between 300 and 380 K are presented in Fig. 2. As it is seen from the figure, the device has a good rectification property and the reverse bias current of the junction strongly depends on temperature. To analyze the electrical properties of the device in dark, the well known thermoionic emission theory can be used. According to the theory, the net current across to the structure can be written as [25]

$$I = I_0 \exp\left(\frac{qV}{nkT}\right)\left[1 - \exp\left(-\frac{qV}{kT}\right)\right] \quad (1)$$

where I_0 is the reverse saturation current, q the electronic charge, V the applied voltage, k the Boltzmann constant, T the absolute temperature and n the ideality factor. The ideality factor of the device was determined between 1.68 and 1.54 from the slope of the linear region of forward bias *I–V* plots (Fig. 2). The calculated results are given in Table 1. The obtained n value of the device greater than unity implies deviation from ideal diode. This deviation may be due to the series resistance and the presence of surface states in ZnO [18]. Yakuphanoglu [18] calculated the ideality factor of Au/ZnO:Co/n-Si device obtained by using sol–gel deposition of Co-doped ZnO (ZnO:Co) film on n-type silicon as 2.79. Ghosh et al. [26] obtained SnS/ZnO heterojunction using electrodeposited ZnO film and determined the ideality factor of the junction to be 1.28. In addition, as seen from Table 1 the ideality factor decreases with the increase in temperature. Similar results for metal–semiconductor (MS) contacts and metal–interlayer–semiconductor (MIS) have been reported [27–31].

The saturation current of a device is given by the following equation

$$I_0 = AA^*T^2 \exp\left(-\frac{q\phi_b}{kT}\right) \quad (2)$$

where A is the diode contact area, A^* the Richardson constant equals to 36 A cm^{-2} K^{-2} for ZnO [32] and ϕ_b the barrier height. The barrier height of the Al/ZnO/p-InP heterojunction was calculated between 0.81 and 0.90 eV from the reverse saturation current values obtained from Fig. 2 by the help of Eq. (2). Since current transport across the MS interface is a temperature activated process, electrons at low temperatures are able to surmount the lower barriers and therefore, the current transport will be dominated by current flow through the patches of lower Schottky barrier height and a larger ideality factor. As the temperature increases, more and more electrons have sufficient energy to surmount the higher barrier [27,33,34]. As a result, the saturation current and the dominant barrier height increase and the ideality factor decreases with increasing the temperature.

The forward bias *I–V* plots of the diode deviate from linearity at high voltages because of the series resistance. Norde functions can be used to determine the series resistance of the device using forward bias *I–V* data. Norde's method is defined by following relation

Table 1
Electrical parameters of Al/ZnO/p-InP heterojunction between 300 and 380 K obtained from its *I–V* measurements.

Temperature	ln *I–V*		Norde			
	n	ϕ_b (eV)	$F(V_0)$ (V)	V_0 (V)	ϕ_b (eV)	R_s (kΩ)
300	1.68	0.81	0.794	0.109	0.82	11.14
320	1.64	0.83	0.810	0.090	0.83	8.87
340	1.60	0.85	0.835	0.096	0.85	6.33
360	1.56	0.87	0.862	0.086	0.87	4.23
380	1.54	0.90	0.888	0.085	0.90	2.30

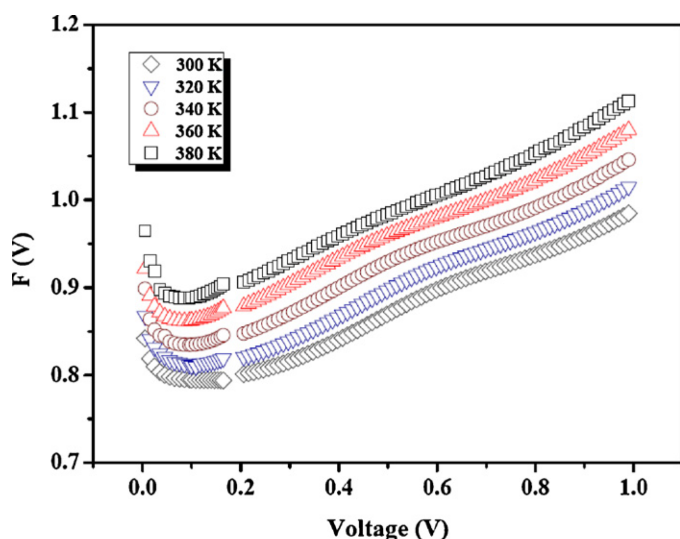

Fig. 3. The $F(V)$ vs. V plots for the Al/ZnO/p-InP heterojunction.

[35,36]

$$F(V) = \frac{V_0}{\gamma} - \frac{kT}{q}\left(\frac{I(V)}{AA^*T^2}\right) \quad (3)$$

where γ is the first integer greater than ideality factor and $I(V)$ the current obtained from I–V characteristics. In this study, all n values are between 1 and 2 and γ is taken as 2 for Al/ZnO/p-InP diode. The $F(V)$ vs. V plots for the diode is given in Fig. 3. The barrier height of the device can be expressed as

$$\phi_b = F(V_0) + \frac{V_0}{\gamma} - \frac{kT}{q} \quad (4)$$

where $F(V_0)$ is the minimum value of $F(V)$ and V_0 is the corresponding voltage value. The R_s of the diode is calculated through the relation

$$R_s = \frac{kT(\gamma - n)}{qI_0} \quad (5)$$

The barrier height values of the junction increase from 0.82 to 0.90 eV between 300 and 380 K. The barrier height values of the heterojunction obtained from Norde's equations are in good agreement with the ones obtained from ln I–V plots. The series resistances of the device decrease from 11.14 kΩ to 2.3 kΩ in the same temperature interval. The increase of R_s with the fall of temperature can be attributed to the increase of n and lack of free carrier concentration at low temperatures [27,37].

3.2. Photovoltaic properties of ZnO/p-InP structure

To see the effect of light, I–V properties of the diode in dark and under 100 mW/cm^2 are shown in Fig. 4a. As seen from the figure the ZnO/p-InP heterojunction has a very strong light sensitivity and the reverse bias current increases about 2000 times at −1 V. The photovoltaic properties of a solar cell can be analyzed using its current density–voltage (J–V) properties. The J–V measurements were taken under 40, 60, 80 and 100 mW/cm^2 illumination conditions to see the effects of light intensity and presented in Fig. 4b. The photocurrent density of the cell increases from 171 to 437 μA/cm^2 and the open circuit voltage increases (V_{oc}) from 477 to 523 mV when the light intensity is increased 40–100 mW/cm^2. Moreover, the photovoltaic properties of the cell were determined using the J–V data obtained under the light with 100 mW/cm^2 and AM1.5 filter. The solar power conversion efficiency (η) and the fill factor (FF) of the cell can be determined using equations [38]

$$\eta = \frac{V_m x J_m}{P_{in}} \quad (6)$$

where

$$FF = \frac{V_m x J_m}{V_{oc} x I_{sc}} \quad (7)$$

where J_m is the current density and V_m the voltage at maximum power point under the light, V_{oc} the open circuit voltage and I_{sc} the closed circuit current. Table 2 presents all photovoltaic parameters of ZnO/p-InP solar cell at 100 mW/cm^2 and AM1.5 filter. Photovoltaic properties of some ZnO/n-InP heterojunctions fabricated

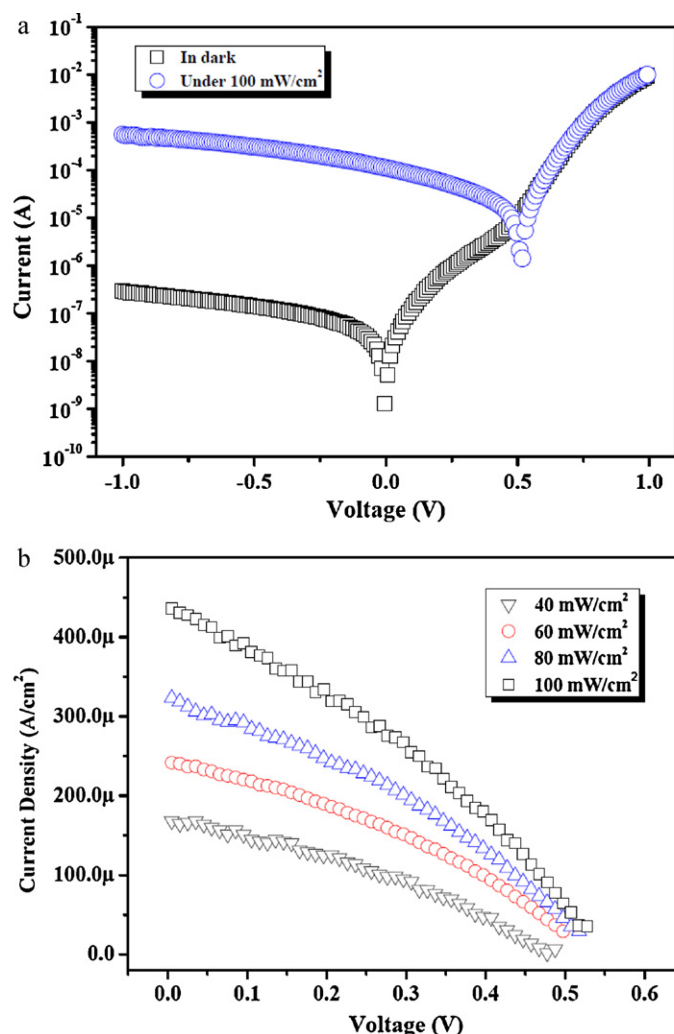

Fig. 4. (a) I–V properties of the ZnO/p-InP cell in dark and under 100 mW/cm^2. (b) J–V measurements of the ZnO/p-InP cell under 40, 60, 80 and 100 mW/cm^2 illumination.

Table 2
Photovoltaic parameters of ZnO/p-InP heterojunction.

Cell parameters	Values under 100 mW/cm^2 and AM1.5 illumination
I_{sc} (μA)	101
V_{oc} (mV)	523
I_m (μA)	58
V_m (mV)	297
FF	0.32
η (%)	0.0754
Cell area	0.23 cm^2

using different methods have been analyzed by different authors [4,39,40]. For instance, Purica et al. [4] have formed ZnO/p-InP heterojunction by the ZnO thin film deposition on p-InP epitaxial layer by the decomposition of metaloorganic compounds as Zn acetylacetonate. They have analyzed the photovoltaic properties of the junction under 1 kl× light intensity and found V_{oc} and I_{sc} values as 0.52 V and 120 μA, respectively. Pande and Manikopoulos [40] fabricated ZnO-p-InP heterojunctions by means of a reactive evaporation technique for the deposition of ZnO. They formed ZnO layer by evaporating Zn in oxygen at 10 mTorr and annealing the structure in Argon atmosphere. The cells had a high efficiency (6.6%) and low series resistance (30 Ω). Under air mass one illumination the cells exhibit a photovoltaic effect with an open-circuit voltage of 0.56 V, a short-circuit current of 19.3 mA cm^{-2} and a fill factor of 0.61. When the results are compared with these studies, it is seen that the V_{oc} values of ZnO/p-InP are very close to each other and the I_{sc} values are very different. The difference in I_{sc} values can be attributed to the effects of series resistance values of the devices which may depend on ZnO formation method and the bulk resistance of ZnO layers.

4. Conclusions

A 50 nm ZnO thin film was formed on p-InP wafer to analyze the electrical properties of ZnO/p-InP heterojunction. The ideality factor, barrier height and series resistance of the heterojunction were determined using its current–voltage (*I*–*V*) measurements between 300 and 380 K with 20 K intervals. It was seen that the barrier height of ZnO/p-InP device increased and ideality factor and series resistance of the structure reduced while the temperature was increased. In addition, the effect of light on electrical properties of the device was examined between 40 and 100 mW/cm^2 with 20 mW/cm^2 intervals. The photovoltaic parameters of the device were determined under 100 mW/cm^2 and AM1.5 illumination condition and it was observed that the cell had power conversion efficiency and fill factor as % 0.0754 and 0.32 values, respectively.

References

[1] W.W. Zhong, F.M. Liu, L.G. Cai, C.C. Zhou, P. Ding, H. Zhang, J. Alloys Compd. 499 (2010) 265–268.
[2] M. Benhaliliba, C.E. Benouis, M.S. Aida, A.S. Juarez, F. Yakuphanoglu, A.T. Silver, J. Alloys Compd. 506 (2010) 548–553.
[3] H.X. Liu, B.B. Huang, Z.Y. Wang, X.Y. Qin, X.Y. Zhang, J.Y. Wei, Y. Dai, P. Wang, M.H. Whangbo, J. Alloys Compd. 507 (2010) 326–330.
[4] M. Purica, E. Budianu, E. Rusu, Thin Solid Films 383 (2001) 284–286.
[5] X.L. Xu, S.P. La, J.S. Chen, G.Y. Chen, B.K. Tay, J. Cryst. Growth 223 (2001) 201–205.
[6] Y. Caglar, S. Ilican, M. Caglar, F. Yakuphanoglu, J. Wu, K. Gao, P. Lu, D. Xue, J. Alloys Compd. 481 (2009) 885–889.
[7] J.H. Kim, D.H. Cho, W. Lee, B.M. Moon, W. Bahng, S.C. Kim, N.K. Kim, S.M. Koo, J. Alloys Compd. 489 (2010) 179–182.
[8] D.K. Kim, H.B. Kim, J. Alloys Compd. 509 (2011) 421–425.
[9] Y. Imanishi, M. Taguchi, K. Onisawa, Thin Solid Films 518 (2010) 2945–2948.
[10] R.I. Badran, A. Umar, S. Al-Heniti, A. Al-Hajry, T. Al-Harbi, J. Alloys Compd. 508 (2010) 375–379.
[11] M. Caglar, S. Ilican, Y. Caglar, F. Yakuphanoglu, J. Alloys Compd. 509 (2011) 3177–3182.
[12] E. Bacaksiz, S. Aksu, S. Yılmaz, M. Parlak, M. Altunbaş, Thin Solid Films 518 (2010) 4076–4080.
[13] Y. Li, L. Xu, X. Li, X. Shen, A. Wang, Appl. Surf. Sci. 256 (2010) 4543–4547.
[14] C.Y. Tsay, K.S. Fan, S.H. Chen, C.H. Tsai, J. Alloys Compd. 495 (2010) 126–130.
[15] C. Yan, D. Xue, L. Zou, J. Alloys Compd. 453 (2008) 87–92.
[16] S.K. Sharma, A.I. Inamdar, Hyunsik Im, B.G. Kim, P.S. Patil, J. Alloys Compd. 509 (2011) 2127–2131.
[17] S.W. Hwang, J.H. Seo, T.H. Yoon, J.C. Kim, Thin Solid Films 519 (2010) 885–889.
[18] F. Yakuphanoglu, J. Alloys Compd. 494 (2010) 451–455.
[19] T.F. Lei, W.C. Huang, L.C. Len, J. Appl. Phys. 78 (1995) 6108–6112.
[20] Z.J. Horwath, V. Rakovics, B. Szentpali, S. Puspoki, Phys. Status Solidi (c) 0 (3) (2003) 916–921.
[21] M. Soylu, B. Abay, Y. Onganer, J. Phys. Chem. Solids 71 (2010) 1398–1403.
[22] S. Darwish, I.K. El Zawawi, A.S. Riad, Thin Solid Films 485 (2005) 182–187.
[23] Y. Sun, A. Yulius, G. Li, J.M. Woodall, Solid State Electron. 48 (2004) 1975–1979.
[24] O. Gullu, A. Turut, Sol. Energy Mater. Sol. Cells 92 (2008) 1205–1210.
[25] E.H. Rhodreick, R.H. Willimas, Metal–Semiconductor Contacts, second ed., Clarendon Press, Oxford, 1988.
[26] B. Ghosh, M. Das, P. Banerjee, S. Das, Semicond. Sci. Technol. 24 (2009) 025024.
[27] Y.S. Ocak, M.A. Ebeoglu, G. Topal, T. Kılıcoglu, Physica B 405 (2010) 2329–2333.
[28] A.A.M. Farag, E.A.A. El-Shazly, M. AbdelRafea, A. Ibrahim, Energy Mater. Sol. Cells 93 (2009) 1853–1859.
[29] H. Korkut, N. Yildirim, A. Turut, Microelectron. Eng. 86 (2009) 111–116.
[30] B. Abay, J. Alloys Compd. 506 (2010) 51–56.
[31] M.B. Reddy, A.A. Kumar, V. Janardhanam, V.R. Reddy, P.N. Reddy, Curr. Appl Phys. 9 (2009) 972–977.
[32] O. Madelung, M. Schulz, H. Weiss, Semimagnetic Semiconductors, Landolt–Bornstein, New, Series, Group III, Part B, vol. 17, Springer, Berlin, 1982.
[33] S. Gupta, D. Patidar, M. Baboo, K. Sharma, N.S. Saxena, Front. Optoelectron. China 3 (2010) 321–327.
[34] S. Altindal, B. Sari, H.I. Unal, N. Yavas, J. Appl. Polym. Sci. 113 (2009) 2955–2961.
[35] H. Norde, J. Appl. Phys. 50 (1979) 5052–5053.
[36] I.S. Yahia, M. Fadel, G.B. Sakr, F. Yakuphanoglu, S.S. Shenouda, W.A. Farooq, J. Alloys Compd. 509 (2011) 4414–4419.
[37] S. Chand, J. Kumar, Appl. Phys. A 63 (1996) 171–178.
[38] S.J. Fonash, Solar Cell Device Physics, second ed., Elsevier, 2010.
[39] E. Rusu, M. Purica, E. Budianu, S. Nan, Proceedings of the International Semiconductor Conference – CAS, Sinaia, Romania, 1998, pp. 515–518.
[40] K.P. Pande, C.N. Manikopoulos, Sol. Cells 4 (1981) 147–152.